RESEARCH ARTICLE

Citrus flavonoid 5-demethylnobiletin suppresses scavenger receptor expression in THP-1 cells and alters lipid homeostasis in HepG2 liver cells

Jui-Hung Yen[1], Ching-Yi Weng[2]*, Shiming Li[3], Ya-Hsuan Lo[2], Min-Hsiung Pan[4], Shih-Hang Fu[2], Chi-Tang Ho[3] and Ming-Jiuan Wu[2]*

[1] Department of Molecular Biology and Human Genetics, Tzu Chi University, Hualien, Taiwan
[2] Department of Biotechnology, Chia Nan University of Pharmacy and Science, Tainan, Taiwan
[3] Department of Food Science, Rutgers University, New Brunswick, NJ, USA
[4] Department of Seafood Science, National Kaohsiung Marine University, Kaohsiung, Taiwan

Received: May 18, 2010
Revised: October 23, 2010
Accepted: November 5, 2010

Scope: Nobiletin, a polymethoxyflavone from the peel of citrus fruits, has been reported to inhibit modified LDL uptake in macrophages and enhance hepatic LDL receptor expression and activity. We report the anti-atherogenic effect and mechanism of 5-demethylnobiletin, an auto-hydrolysis product of nobiletin.

Methods and results: 5-Demethylnobiletin significantly attenuated phorbol 12-myristate 13-acetate-induced gene expression and activity of scavenger receptors, CD36, scavenger receptor-A and lectin-like oxidized LDL receptor-1. The inhibitory effect is partly associated with the inhibition of protein-kinase C activity and c-Jun NH_2-terminal kinase 1/2 phosphorylation, thereby inhibiting the activation of activator protein-1 and nuclear factor-κB. 5-Demethylnobiletin treatment also led to reduction of oxidized LDL-induced CD36 mRNA expression and blockade of 1,1′-dioctadecyl-3,3,3′,3′-tetramethylindocarbocyanide perchlorate-modified LDL uptake in THP-1-derived macrophages. In the human hepatoma cell line HepG2, 5-demethylnobiletin significantly induced LDL receptor activity and transcription, at least in part, through steroid-response element-binding protein-2 activation. 5-Demethylnobiletin also decreased the mRNA expression of acyl CoA:diacylglycerol acyltransferase 2, the key enzyme involved in the hepatic triacylglycerol biosyntheses.

Conclusion: Current results suggest that 5-demethylnobiletin has diverse anti-atherogenic bioactivities. It is more potent in inhibiting monocyte-to-macrophage differentiation and foam cell formation than its permethoxylated counterpart, nobiletin. It exhibits similar hypolipidemic activity as nobiletin and both can enhance LDL receptor gene expression and activity and decreased acyl CoA:diacylglycerol acyltransferase 2 expression.

Keywords:
Acyl CoA:diacylglycerol acyltransferase 2 / Atherogenesis / CD36 / c-Jun NH_2-terminal kinase / Steroid-response element-binding protein-2

Correspondence: Professor Ming-Jiuan Wu, Department of Biotechnology, Chia Nan University of Pharmacy and Science, Tainan 717, Taiwan
E-mail: imwu@mail.chna.edu.tw
Fax: +886-6-266-2135

Abbreviations: acLDL, acetylated LDL; **apoB,** apolipoprotein B; **AP-1,** activator protein-1; **DGAT,** acyl CoA:diacylglycerol acyltransferase; **3′,4′-didemethylnobiletin,** 3′,4′-dihydroxy-5,6,7,8-tetramethoxyflavone; **DiI,** 1,1′-dioctadecyl-3,3,3′,3′-tetramethylindocarbocyanide perchlorate; **EMSA,** electrophoretic mobility shift assay; **ERK,** extracellular signal-regulated kinase; **GAPDH,** glyceraldehyde 3-phosphate dehydrogenase; **HMG-CoA,** 3-hydroxy-3-methyl-glutaryl-CoA; **JNK,** c-Jun NH_2-terminal kinase; **LDLR,** LDL receptor; **LOX-1,** lectin-like oxidized LDL receptor-1; **MAPK,** mitogen-activated protein kinase; **NF-κB,** nuclear factor-κB; **NOB,** nobiletin; **oxLDL,** oxidized LDL; **PKC,** protein-kinase C; **PMA,** phorbol 12-myristate 13-acetate; **PMF,** polymethoxyflavone; **SR,** scavenger receptor; **SRE,** sterol-regulatory element; **SREBP,** steroid-response element-binding protein

*These authors contributed equally to this work.

1 Introduction

Atherosclerosis, which is characterized by an accumulation of lipid laden foam cells beneath the aortic endothelium, constitutes the single most important contributor to cardiovascular disease [1]. Plasma LDL readily enters the artery wall by crossing the endothelial membrane into intima, where it is subjected to a variety of modifications. The modified LDL activates endothelial cells to express monocyte chemotactic protein 1, which attracts monocytes from the vessel lumen into the subendothelial space [2] and promotes the differentiation of monocytes into macrophages [1]. The activated macrophages in turn release a variety of inflammatory cytokines and express high level of scavenger receptors (SRs) which recognize and uptake the different forms of modified LDL and lead to the formation of foam cells [1]. A variety of SRs have been identified, and CD36, SR-A, and lectin-like oxidized LDL receptor-1 (LOX-1) represent the principal receptors in the process of foam cell formation [3, 4]. The direct evidences of the involvement of SRs in atherosclerosis have been demonstrated using knockout mice [5–10] and these findings suggest that CD36, SR-A, and LOX-1 play pro-atherogenic roles *in vivo*.

It is well known that the liver not only manufactures and secretes VLDL into the blood but also removes LDL from the blood. The regulation of plasma LDL cholesterol levels *via* LDL receptor (LDLR)-mediated clearance is a well-defined process involving endocytosis and lysosomal degradation of LDL. Increased hepatic LDLR expression results in improved removal of LDL cholesterol and is associated with a decreased risk of developing cardiovascular diseases [11]. Therapeutic interventions that increase hepatic LDLR expression could improve LDL clearance from the circulation and in turn slow atherosclerotic development and reduce the risk of coronary heart disease [12, 13].

Hepatic overproduction of apolipoprotein B (apoB)-containing lipoprotein is among the most prevalent complications associated with high risk of developing atherosclerosis [14]. The synthesis and availability of triacylglycerols play a critical role in intracellular apoB processing and secretion of VLDL [15]. As a result, modulation of hepatic triacylglycerol synthesis and associated key enzyme activities may serve as pharmacological targets for lowering plasma lipoprotein level. Acyl CoA:diacylglycerol acyltransferases (DGATs) are microsomal enzymes that catalyze the last committed step in triacylglycerol synthesis. DGAT1 and DGAT2 are the two DGAT proteins, which have distinct tissue distribution: the former is expressed most highly in the enterocytes, whereas the latter has high expression in the hepatic and adipose tissue [16].

The roles of citrus flavonoids in prevention and treatment of disease have recently received considerable attention, with particular interest in the use of these flavonoids as anti-inflammatory, anti-cancer, and anti-atherogenic agents [17]. Animal experiments and clinical trials showed that oral administration of citrus flavonoids significantly decreased the level of cholesterol and triglycerides [18–23]. The molecular mechanisms underlying the hypolipidemic effects of citrus flavonoids have been attributed to upregulated expression of LDLR [24] as well as reduced activities or expressions of a number of lipogenic enzymes, including DGATs [25], 3-hydroxy-3-methyl-glutaryl-CoA (HMG-CoA) reductase [20], acyl CoA:cholesterol acyl-CoA:cholesterol acyltransferase and microsomal triglyceride transfer protein [26].

In addition to the noted hypolipidemic potential, oral administration of citrus flavonoids could decrease aortic fatty streak area in high cholesterol-fed rabbits [27]. Cell-culture data demonstrated that nobiletin (NOB), a citrus polymethoxyflavone (PMF), inhibited acetylated LDL (acLDL) uptake in J774A.1 macrophages [28] and SR expression in phorbol 12-myristate 13-acetate (PMA)-induced THP-1 cells [29, 30]. Recently, our laboratory also demonstrated that 3′,4′-dihydroxy-5,6,7,8-tetramethoxyflavone (3′,4′-didemethylnobiletin), a metabolite of NOB, inhibited both PMA- and oxidized LDL (oxLDL)-induced monocyte differentiation and modified LDL uptake in macrophages [31].

NOB (Fig. 1) is one of the most studied and abundant PMFs found in orange peel extract from cold-pressed sweet orange peel oil [32]. 5-Demethylnobiletin (Fig. 1) can be isolated from aged orange peel extract, and is believed to be formed by auto-hydrolysis of NOB during long-term storage [33–35]. Recently, efforts have been made to compare the biological activities of hydroxylated PMFs with their permethoxylated counterparts. It was found that 5-demethylnobiletin exhibited much stronger inhibitory effects on the growth of various cancer cells in comparison with NOB, suggesting the pivotal role of hydroxyl group at the 5-position in the enhanced anti-cancer activity [33–36].

Although the aforementioned studies demonstrated promising effects of citrus flavonoids, such as naringin, naringenin, hesperetin, and NOB, on prevention of atherosclerosis, to the best of our knowledge, no study has been conducted for 5-demethylnobiletin. As a consequence, we aim to understand whether 5-demethylnobiletin possesses anti-atherogenic activity and its underlying mechanism. Our effort was focused on the regulatory effects of 5-demethylnobiletin on monocyte-to-macrophage differentiation, foam cell formation, hepatic LDLR activity and expression, and hepatic DGAT2 expression. It is noteworthy that this is the first report on the anti-atherosclerotic effect and mechanism of 5-demethylnobiletin.

2 Materials and methods

2.1 Materials

5-Demethylnobiletin, NOB, and 3′,4′-didemethylnobiletin were purified or synthesized as described earlier (Fig. 1) [37]. RPMI-1640 medium, PMA, and other chemicals were

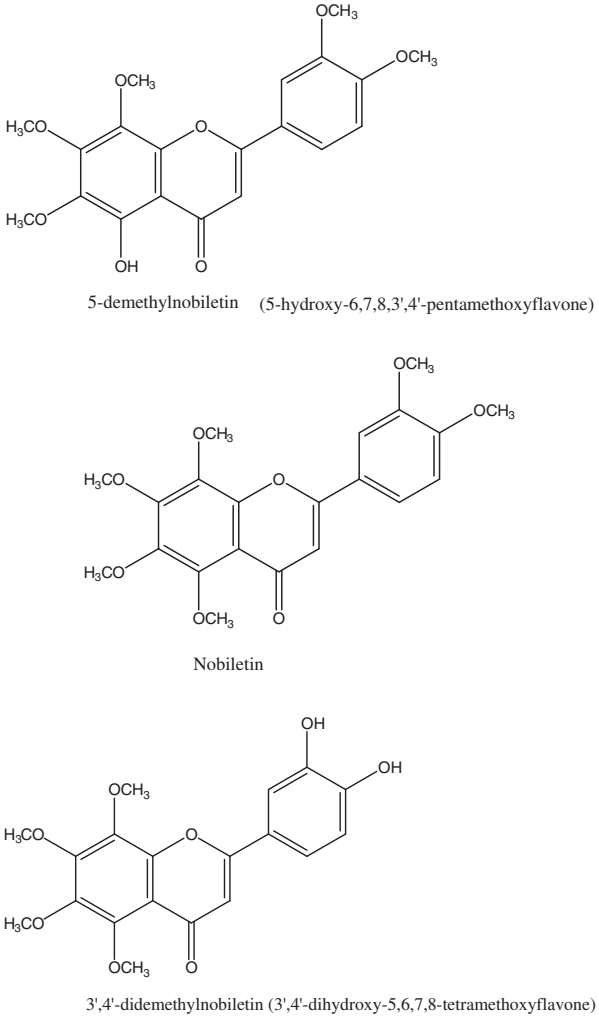

Figure 1. Chemical structures of 5-demethylnobiletin, NOB, and 3′,4′-didemethylnobiletin.

purchased from Sigma-Aldrich (St. Louis, MO, USA) unless otherwise stated. Fetal bovine serum was purchased from Hyclone (Logan, UT, USA). 1,1′-Dioctadecyl-3,3,3′,3′-tetramethylindocarbocyanide perchlorate (DiI) was purchased from Invitrogen Life Technologies (Carlsbad, CA, USA).

2.2 Preparation and oxidation of LDL

LDL ($d = 1.019$–1.063 g/mL) was prepared from the plasma of healthy donors by sequential ultracentrifugation [38]. Lipoprotein was desalted and concentrated by ultra-filtration (Centricon 4, Amicon, Beverly, MA, USA) against PBS at $450 \times g$, 4°C for 120 min. The protein concentration was measured by the method of Bradford [39], using BSA as a standard.

Briefly, oxLDL was prepared by incubation of LDL (0.2 mg of LDL protein/mL) with 5 μM Cu^{2+} in PBS at 37°C for 24 h, followed by addition of 0.24 mM EDTA to stop oxidation. The degree of LDL oxidation was determined by measurement of TBARS formation [40]. In all, oxLDL was sterilized by filtration through a 0.45 μm pore size filter (Gelman Sciences, Ann Arbor, MI) and stored at 4°C.

2.3 Preparation of DiI-LDL, DiI-oxLDL, and DiI-acLDL

LDL was incubated overnight at 37°C under nitrogen and light protection with 50 μL of DiI (3 mg/mL in DMSO) for each milligram of LDL protein. The LDL must be labeled before acetylation or oxidation [41]. For preparation of DiI-oxLDL, DiI-LDL (0.2 mg/mL) was incubated with 5 μM Cu^{2+} in PBS at 37°C in dark for 24 h [42]. Unbound dye and copper ions from the oxidation step which would otherwise be toxic to the cells were removed by passing through Sephadex G-25 (GE Healthcare, Buckinghamshire, UK). For preparation of DiI-acLDL, the method described by Basu *et al.* [43] was employed. Unbound dye and acetic anhydride from acetylation step were then removed by passing through Sephadex-G25. Protein concentration of elute was determined by Bradford [39]. All lipoprotein preparations were stored at 4°C in sterile containers after filtration sterilization (0.45 μm).

2.4 Treatment of THP-1 cells with flavonoids

The monocyte-like cell line THP-1 was obtained from Bioresource Collection and Research Center (Hsinchu, Taiwan). THP-1 cells were cultured in RPMI 1640 medium, which contained 0.3 g/L L-glutamine, 4.5 g/L glucose, 10 mM HEPES, 1.0 mM sodium pyruvate, and 10% fetal bovine serum. Cell cultures were maintained at 37°C in a humidified 5% CO_2/95% air incubator.

For monocytic-to-macrophage differentiation, THP-1 monocytes were cultured in 6-well plates (1×10^6 cells/mL) in RPMI-1640 medium for 30 min with test sample at the specified concentrations, or with the vehicle (0.1% DMSO, v/v), followed by stimulation with 30 nM PMA for 24 h. DiI-modified LDL uptake or SR expression was then measured as described below.

To prepare THP-1-derived macrophages, THP-1 monocytes were cultured in 6-well plates (1×10^6 cells/mL) supplemented with PMA (200 nM) for 72 h. Nonadherent cells were then removed by washing the wells twice with medium. Macrophages were then treated with test sample or control vehicle and cultured for additional 48 h in fresh medium. DiI-modified LDL uptake or mRNA expression of SRs was then measured as described below.

2.5 Treatment of HepG2 cells with flavonoids

HepG2 cells from the Bioresource Collection and Research Center were maintained at 37°C, 5% CO_2 in DMEM

supplemented with 10% fetal bovine serum, 2 mM glutamine, 1% nonessential amino acids, 1 mM pyruvate, 100 U/mL penicillin, and 100 μg/mL streptomycin (Gibco BRL, NY, USA).

For measurement of the mRNA expression of LDLR, HMG-CoA reductase, and DGAT2, as well as SREBP-2 (SREBP, steroid-response element-binding protein) processing, HepG2 cells (1×10^6 cells/mL) were seeded in 6-well plates in normal medium for 24 h, followed by compound treatment for additional 24 h [24]. For DiI-LDL uptake analysis, attached HepG2 cells (1×10^6 cells/mL) were changed to serum-free medium for overnight followed by compound treatment for additional 24 h [44].

2.6 Cell viability analysis

To examine cytotoxicity of 5-demethylnobiletin during monocyte-to-macrophage differentiation, THP-1-derived macrophages or HepG2 cells, 3-(4,5-dimethylthiazol-2-yl)-2,5-diphenyltetrazolium assay was used [45]. The concentrations employed in the experiments did not exert significant cytotoxicity (cell viability $>90\%$).

2.7 DiI-LDL uptake measurement

DiI-modified LDL and DiI-LDL (10 μg/mL) was added into THP-1 cells and HepG2 cells, respectively, and incubated for 24 h. The cells were washed with PBS and then examined with a fluorescence-inverted microscope (IX-71, Olympus) followed by flow cytometry analysis (FACScan, BD Biosciences, San Jose, CA, USA) using the FL2 emission filter. Data were acquired from 10 000 cells (events), and the uptake was determined and expressed as the geometric mean fluorescence intensity.

2.8 mRNA expression of SR-A, CD36, LOX-1, CD11b, LDLR, HMG-CoA reductase, and DGAT2

Total cellular RNA was prepared using Illustra RNAspin Mini RNA Isolation Kit (GE Healthcare). Reverse-transcription was carried out using 1 μg RNA and High-Capacity cDNA Archive kit (Applied Biosystems, Foster City, CA, USA). Quantitative PCR was performed with 2 μL cDNA obtained above in 25 μL containing 200 nM primers using Power SYBR® Green PCR Master Mix (Applied Biosystems). The primer sequences were deduced from PrimerBank [46] and listed in Supporting Information Table 1. Amplification was conducted on the ABI Prism 7300 sequence detection system. PCR conditions were as follows: 95°C for 2 min, 40 cycles at 95°C for 15 s, and 60°C for 45 s. The optimal concentrations of primers and templates used were established based on the standard curve created before the reaction and corresponded to approximately 100% reaction efficiency. PCR results were then normalized to the expression of glyceraldehyde 3-phosphate dehydrogenase (GAPDH) in the same samples.

2.9 Electrophoretic mobility shift assay for nuclear factor-κB and activator protein-1 activation analysis

HP-1 cells (6×10^6 cells/6 mL in a 100-mm dish) were incubated with the indicated agent or vehicle (0.1% DMSO, v/v), stimulated with PMA (30 nM), then and collected after 4 h. Nuclear protein was isolated using NE-PER nuclear and cytoplasmic extraction reagents (Thermo Scientific, Rockford, IL, USA). Briefly, 12 μg of nuclear protein was incubated with 50 fmol of 5′-biotinate double-stranded oligonucleotide probes containing a consensus binding-sequence for nuclear factor-κB (NF-κB) (5′-AGTTGAGGGGACTTTCCCAGGC-3′) or activator protein-1 (AP-1) (5′-TTCGGCTGACTCATCAAGCG-3′) [47] for 30 min at room temperature and resolved in an 8% nondenaturing polyacrylamide gel at 4°C. The protein–DNA–biotin complexes were blotted onto a nylon membrane followed by UV cross-linking. The complexes were revealed with streptavidin-horseradish peroxidase conjugate and substrate (LightShift Chemiluminescent EMSA Kit, Thermo Scientific). Specificity of the DNA–protein complex was confirmed by competition with 100-fold excess of an unlabeled NF-κB or AP-1 probe.

2.10 Extracellular signal-regulated kinase 1/2, c-Jun NH_2-terminal kinase 1/2, and p38 mitogen-activated protein kinase immunoblotting

THP-1 cells (6×10^6 cells/6 mL in a 100-mm dish) were incubated with the indicated agent or vehicle (0.1% DMSO, v/v), stimulated with PMA (30 nM), then and collected after indicated time. Cells were rinsed in PBS before lysing with RIPA buffer (Thermo Scientific), with protease inhibitor cocktail (Sigma-Aldrich) and phosphatase inhibitor cocktail (Calbiochem, San Diego, CA, USA), according to the recommendations of the suppliers. Cell lysates (20 μg/lane) were resolved by 8% SDS-PAGE and transferred onto Hybond ECL nitrocellulose (GE Healthcare) at 20 V overnight at 4°C. The membranes were blocked at room temperature in blocking buffer (5% BSA in PBS solution) for 2 h. Blots were analyzed with each antibody at a dilution of 1:1000 anti-ERK1/2 (ERK, extracellular signal-regulated kinase) (clone 137F5), anti-JNK1/2 (JNK, c-Jun NH_2-terminal kinase) (clone 56G8), anti-p38, anti-phospho-ERK1/2 (clone D13.14.4E), anti-phospho-JNK1/2 (clone 81E11), and anti-phospho-p38 (clone 3D7) (Cell Signaling Technology, Beverly, MA, USA) at 4°C for overnight. Peroxidase-conjugated secondary anti-rabbit IgG (1:10 000) were used to detect the proteins of interest by ECL-Plus detection system

(GE Healthcare). The intensities of these bands were analyzed with Phoretix Gel Analysis Software (Nonlinear Dynamics, Newcastle upon Tyne, UK)

2.11 Protein-kinase C kinase activity analysis

A nonradioactive protein-kinase C (PKC) activity assay kit (Enzo Life Sciences, Ann Arbor, MI, USA) was used to evaluate PKC activity in the samples. THP-1 cells (1×10^6 cells/ mL in 6-well plate) were incubated with the indicated agent or vehicle (0.1% DMSO, v/v), stimulated with PMA (30 nM), then and collected after 2 h using lysis buffer according to the manufacturer's instructions. PKC substrate microtiter plate, which was precoated with PKC substrate, was soaked with kinase assay dilution buffer for 10 min at room temperature. In total, 30 μL of cell lysates (50 ng) or PKC standard (10 ng) were then added, followed by the addition of ATP to initiate the reaction. After incubation at 30°C for 90 min, the reaction mixture was removed from the plate, and phosphospecific substrate antibody was added to each well and incubated at room temperature for 60 min. The liquid was aspirated and wells were repeatedly washed. Peroxidase-conjugated secondary anti-rabbit IgG was then added to each well and incubated for another 30 min. The wash was repeated after incubation and TMB substrate solution was added to each well. Stop solution was added after 30–60 min and the 96-well plate was read at 450 nm in a microplate reader.

2.12 SREBP-2 immunoblotting

HepG2 cells (6×10^6 cells/6 mL in a 100-mm dish) were cultured as described above and either lysed on ice in a RIPA buffer for the preparation of total cell lysates, or using NE-PER nuclear and cytoplasmic extraction reagents for the preparation of nuclear extracts. Proteins (30 μg/lane) were analyzed on 8% SDS-PAGE followed by Western blotting analysis with antibodies against C-terminus of SREBP-2 (BD Pharmingen, San Diego, CA, USA) or α-tubulin (Sigma-Aldrich) for total cell lysates; and against N-terminus of SREBP-2 (Cayman, Ann Arbor, MI, USA) or HDAC2 (GeneTex, Irvine, CA, USA) for nuclear extracts according to the manufacturers' suggestions. Blots were developed with the appropriate secondary antibody conjugated to horseradish peroxidase and ECL-Plus detection system (GE Healthcare).

2.13 Statistical analyses

Student's *t*-tests were used to assess significant differences in parameters measured between in the presence and in the absence of test substance. The level of significance was set at $p < 0.05$. All experiments have been performed at least three times.

3 Results

3.1 Effect of 5-demethylnobiletin on SR expression and activity during monocyte-to-macrophage differentiation

To examine whether 5-demethylnobiletin exhibits anti-atherogenic activity, we started with investigating its effect on gene expression associated with the extent of monocyte-to-macrophage differentiation [48]. THP-1 cells were pretreated with noncytotoxic concentration of 5-demethylnobiletin or the vehicle, followed by PMA (30 nM) exposure for 24 h. The mRNA expression of differentiation marker CD11b, and the SRs CD36, SR-A, and LOX-1, was measured by RT-Q-PCR normalized to the level of GADPH and is shown in Fig. 2. CD11b expression was increased by 5.6 ± 0.6-fold when THP-1 monocytes were treated with PMA (30 nM) for 24 h (Fig. 2A). Addition of 5-demethylnobiletin (5–20 μM) in combination with PMA did not appreciably alter CD11b mRNA expression. THP-1 monocytes exhibited very low level of LOX-1 mRNA and the addition of PMA (30 nM) induced a more than 1000-fold increase after 24 h incubation (Fig. 2B). Treatment of THP-1 cells with 5-demethylnobiletin (10–20 μM) attenuated PMA-induced LOX-1 expression by ~45% as compared with PMA-treated cells ($p < 0.01$).

Similarly, THP-1 monocytes exhibited low levels of CD36 and SR-A mRNA, whereas PMA-treated cells induced their expression ~10- and ~400-fold, respectively. THP-1 cells treated with 5-demethylnobiletin (5–20 μM) significantly repressed PMA-stimulated CD36 and SR-A mRNA expression dose dependently. The addition of 20 μM 5-demethylnobiletin almost completely abolished PMA-induced CD36 expression ($p < 0.01$).

Our next approach was to examine whether 5-demethylnobiletin could block modified LDL uptake associated with monocyte differentiation. THP-1 monocytes were pretreated with vehicle or indicated concentration of 5-demethylnobiletin for 30 min prior to exposure to PMA (30 nM) for 24 h. These cells were then incubated with DiI-acLDL (10 μg/mL) for additional 24 h. Accumulation of DiI-acLDL into the cells was observed by fluorescence microscopy (vehicle of Fig. 3A). Addition of 5-demethylnobiletin (5-demethyl NOB, 5 and 10 μM) significantly decreased PMA-induced acLDL uptake. To better quantitate the fluorescence intensity of each cell, flow cytometry was employed as described in Section 2. Figure 3B shows that 5 and 10 μM 5-demethylnobiletin compatibly inhibited DiI-acLDL uptake by about 50%.

We further investigated the structure–activity relationship of citrus flavonoids in the inhibition of PMA-induced gene expression and SR activity by comparing current data with those of permethoxylated and dihydroxylated PMFs, NOB, and 3′,4′-didemethylnobiletin published previously [31]. Supporting Information Table 2 summarizes that NOB decreased only the expression of PMA-induced LOX-1; on

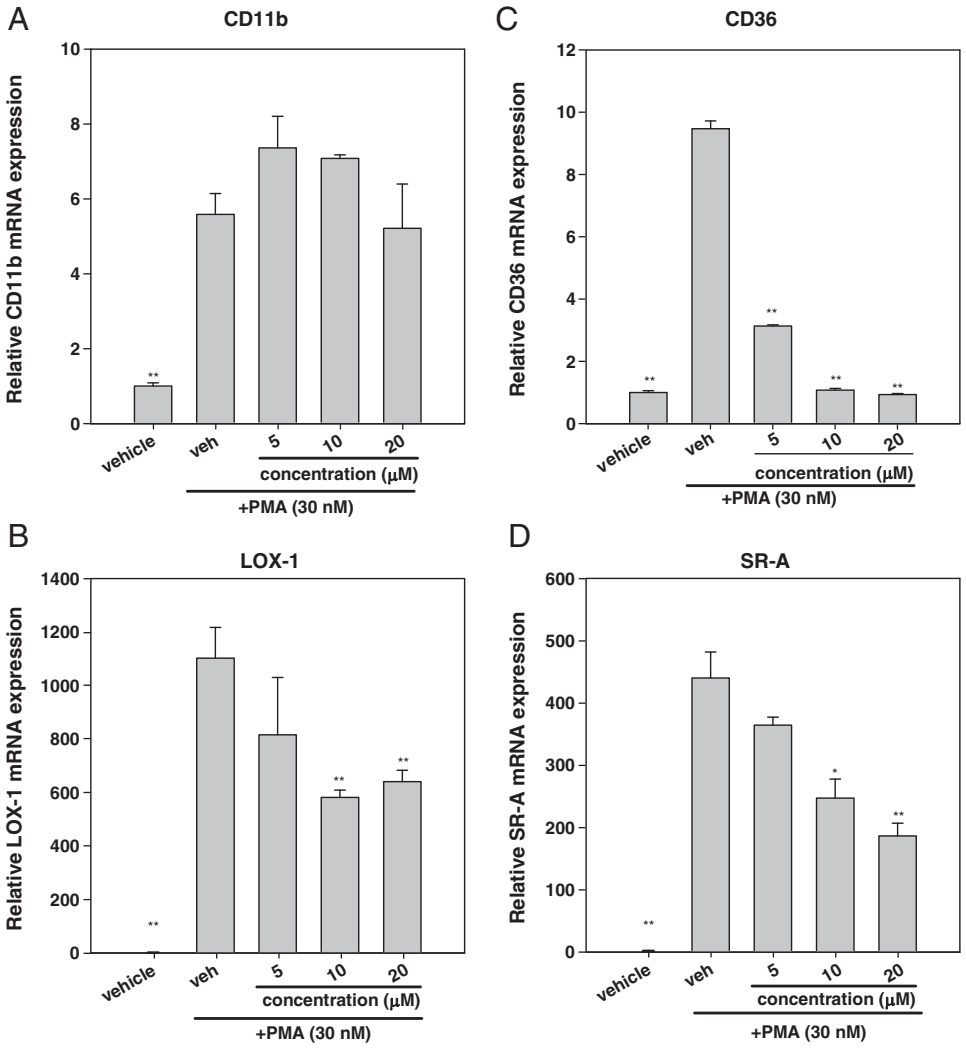

Figure 2. Effect of 5-demethylnobiletin on the mRNA expression of CD11b, LOX-1, CD36, and SR-A during monocyte-to-macrophage differentiation. THP-1 monocytes were treated with vehicle (0.1% DMSO) or 5-demethylnobiletin for 30 min prior to 30 nM PMA addition and incubated for 24 h. Total cellular RNA was prepared and the expression of mRNA was analyzed as described in Section 2. The data were normalized with reference to the expression levels of the corresponding GAPDH mRNAs. Data represent mean ratio $\pm$ SEM of three independent experiments relative to the value of the vehicle. $^{*}p<0.05$ and $^{**}p<0.01$ represent significant differences compared with vehicle plus PMA.

the other hand, 3′,4′-didemethylnobiletin significantly reduced those of SRs and only modestly attenuated that of CD11b. The expression levels of CD36, SR-A, and LOX-1 in 20 μM 3′,4′-didemethylnobiletin-treated cells are relatively low, close to those of monocytes. In addition, the inhibitory activities of 3′,4′-didemethylnobiletin and 5-demethylnobiletin on DiI-acLDL uptake are compatible and better than that of NOB. These results suggest that the presence of hydroxyl group might be important in enhancing inhibitory activity of PMF against PMA-induced gene expression in THP-1 cells.

3.2 Effects of 5-demethylnobiletin on NF-κB and AP-1 activation during monocyte-to-macrophage differentiation

PMA leads to the activation of PKC and subsequently to the activation of NF-κB and AP-1 in THP-1 cells [49, 50]. Putative NF-κB- and AP-1-response elements are found in the promoter region of LOX-1 [51] and the inhibitory effects of NOB and its demethylated metabolites toward PMA-induced SR expression are partly associated with the suppression of NF-κB and AP-1 activation [30]. As a result, it would be intriguing to investigate whether the attenuation of NF-κB or AP-1 activation contributes to the inhibitory activity of 5-demethylnobiletin toward PMA-stimulated SR expression.

Figure 4A shows a representative electrophoretic mobility shift assay (EMSA) gel blot for THP-1 monocytes treated with PMA (30 nM) or in combination with indicated reagent for 4 h. It is found that the PMA-enhanced expression of SR genes was accompanied by a rise of NF-κB DNA-binding activity in nuclear extracts using a biotin-labeled oligonucleotide containing a consensus binding site. The binding was specific since it was inhibited with an excess of unlabeled, identical oligonucleotides, and was absent from the nuclear extract of nonstimulated cells (vehicle). However,

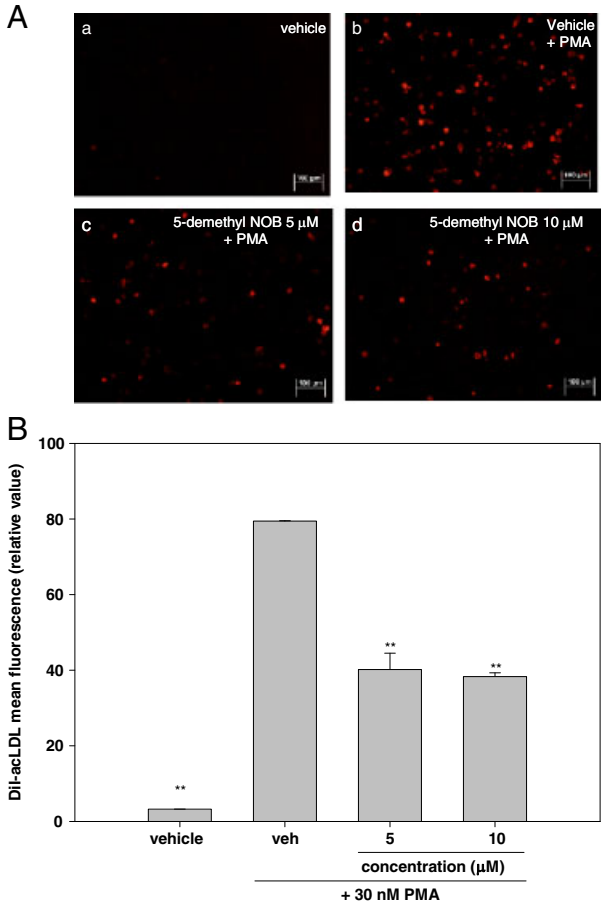

Figure 3. Effect of 5-demethylnobiletin on Dil-acLDL uptake in PMA-stimulated THP-1 monocytes. THP-1 monocytes were treated with vehicle (0.1% DMSO) or the indicated concentration of 5-demethylnobiletin (5-demethyl NOB) for 30 min prior to PMA (30 nM) addition and incubated for 24 h. Dil-acLDL (10 μg/mL) was added to cells and incubated for 24 h. Cell association of Dil-acLDL was observed under fluorescence microscopy (A). Cells were then analyzed by flow cytometry. Data represent mean ratio ± SEM of three independent experiments (B). $^{**}p < 0.01$ represents significant differences compared with vehicle plus PMA.

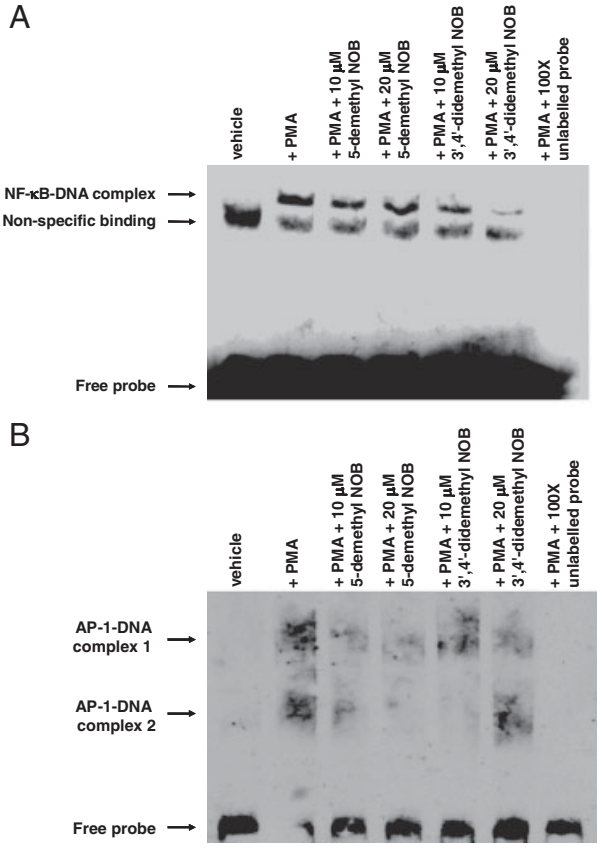

Figure 4. Effect of 5-demethylnobiletin on the activation of NF-κB (A) and AP-1 (B). THP-1 monocytes were incubated with the indicated agent or vehicle (0.1% DMSO, v/v) for 30 min, stimulated with PMA (30 nM), then and collected after 4 h. Nuclear extracts were prepared and NF-κB and AP-1 activities were analyzed by EMSA as described in Section 2.

stimulation cells with PMA for 2 h could not activate NF-κB DNA-binding activity (data not shown). This result is in accordance with the report that PMA induction of NF-κB requires 2–4 h of stimulation and peaks at 4 h in THP-1 cells [52]. PMA-stimulated NF-κB activation was only modestly attenuated by 20–30% by 5-demethylnobiletin, whereas it was strongly inhibited by 40–90% by positive control, 3′,4′-didemethylnobiletin. Figure 4B also shows that stimulation of THP-1 cells with PMA (30 nM) for 4 h slightly stimulated nuclear AP-1-binding activity because AP-1-DNA complexes formed into two smear bands in the representative EMSA gel blot. In contrast to NF-κB activation, the PMA-stimulated AP-1 activation was inhibited more evidently by 5-demethylnobiletin than by 3′,4′-didemethylnobiletin.

3.3 Effects of 5-demethylnobiletin on MAPKs and PKC activation during monocyte-to-macrophage differentiation

NF-κB and AP-1 activation occurs in different cell types in response to a variety of agents (*e.g.* TNF-α, PMA, and LPS), which also play important roles in the activation of MAPKs [53–55]. The impact of 5-demethylnobiletin on the activation of ERK, JNK, and p38 MAPK was thus studied. We pretreated THP-1 cells with vehicle, 5-demethylnobiletin, 3′,4′-didemethylnobiletin, or nobiletin for 30 min and then stimulated them with PMA (30 nM) for 2 h. The total cell lysates obtained were subjected to Western blot analysis to detect both inactive and activated forms of ERK1/2, JNK1/2, and p38 MAPK, using specific antibodies. Figure 5A and B shows that phosphorylated forms of ERK1/2, JNK1/2, and p38 MAPK were all increased by PMA, whereas their respective total protein levels remained unchanged. Exposure to citrus flavonoids markedly suppressed PMA-induced phosphorylation of

JNK, but had no effect on that of ERK. Among them, 10 and 20 μM 5-demethylnobiletin suppressed JNK phosphorylation to the level of vehicle-treated monocytes, whereas 10 and 20 μM 3′,4′-didemethylnobiletin and 20 μM NOB strongly blocked JNK activation to much lower levels. The effect of citrus flavonoids on p38 MAPK activation is distinct. The activation of p38 was further enhanced by 5-demethylnobiletin (10 and 20 μM). However, it was attenuated by NOB (10 and 20 μM) and 3′,4′-didemethylnobiletin (20 μM).

PMA is a structural analogue of diacylglycerol that activates PKC directly both *in vivo* and *in vitro*. Activation of PKC results in the translocation of PKC from the cytosol to the membrane as well as in the phosphorylation of substrate proteins [56]. It is known that PKC activity is required for induction of CD36 by PMA, as well as by PPARγ and RXR ligands [57]. To investigate whether 5-demethylnobiletin interferes with PKC signaling pathways, THP-1 cells were first treated with indicated reagent for 30 min and then stimulated with PMA (30 nM) for 2 h. The cell lysates were prepared and subjected to PKC activity analysis as described in Section 2. Figure 5C shows that treatment of THP-1 monocytes with PMA (30 nM) for 2 h significantly enhanced PKC activity ($p<0.01$). This induction was significantly inhibited by 5-demethylnobiletin (10 μM) and 3′,4′-didemethylnobiletin (10 and 20 μM) but not by NOB. The above data demonstrate that 5-demethylnobiletin and 3′,4′-didemethylnobiletin partially inhibit PKC and JNK1/2 signaling pathways and the activation of nuclear NF-κB and AP-1, which in turn regulate the expression of SRs in PMA-treated THP-1 cells.

3.4 Role of 5-demethylnobiletin in inhibiting foam cell formation in THP-1-derived macrophages

The differentiation of monocytic THP-1 cells into adherent macrophages was achieved by treatment with PMA (200 nM) for 3 days. Cells were then changed to PMA-free medium containing the indicated concentration of 5-demethylnobiletin or control vehicle and cultured for 48 h prior to incubation with DiI-modified LDL (10 μg/mL) for additional 24 h. Flow cytometry analysis demonstrated that the addition of 5-demethylnobiletin (up to 20 μM) exhibited a dose-dependent decrease in DiI-acLDL (Fig. 6A) and DiI-oxLDL uptake (Fig. 6B) by up to 29.8 and 43.0%, respectively, in THP-1-derived macrophages.

To delineate the molecular mechanism by which 5-demethylnobiletin attenuated modified LDL uptake in THP-1-derived macrophages, CD36 and SR-A gene expression was determined, because together these two receptors account for 75–90% of the uptake and degradation of acLDL and oxLDL in macrophages [58]. THP-1-derived macrophages were treated with indicated concentration of 5-demethylnobiletin in the presence or absence of oxLDL (25 μg/mL) for 48 h. The mRNA was then prepared and RT-Q-PCR was performed as described in Section 2. Figure 7 shows that in the absence of oxLDL, neither CD36 nor SR-A transcript was altered by the treatment of 5-demethylnobiletin. In the presence of oxLDL, the expression of CD36 was induced by 1.3-fold as compared with vehicle control and the addition of 5-demethylnobiletin (10–20 μM) strongly inhibited oxLDL-stimulated CD36 expression by 46.6–57.3%. On the other hand, SR-A expression was not appreciably enhanced by oxLDL [59]; nevertheless, 5-demethylnobiletin (10–20 μM) could significantly attenuate SR-A expression by 29.8–39.5% in the presence of oxLDL.

We further compared current findings with those of previously reported for NOB and 3′,4′-didemethylnobiletin [31] and summarized in Supporting Information Table 3. These three citrus flavonoids inhibited oxLDL uptake in macrophages dose dependently and the potency increased in the order of NOB, 5-demethylnobiletin, and 3′,4′-didemethylnobiletin. However, the molecular mechanism that underlies the inhibitory effects of NOB and 3′,4′-didemethylnobiletin seems to differ from that of 5-demethylnobiletin. Both NOB and 3′,4′-didemethylnobiletin are capable of inhibiting CD36 and SR-A mRNA expression in the absence of oxLDL, whereas 5-demethylnobeiletin cannot.

3.5 Effect of 5-demethylnobiletin on LDLR activity and expression in HepG2 cells

The LDLR is responsible for transporting cholesterol-containing lipoprotein particles from the circulation into cells and is expressed predominantly in liver. The expression of LDLR regulates plasma LDL cholesterol homeostasis [11]. It was reported that citrus flavonoids naringenin, hesperetin, and NOB upregulated activity and expression of LDLR in HepG2 cells [24, 26]. To investigate whether 5-demethylnobiletin would also change the cholesterol homeostasis, we first evaluated its effect on LDLR activity in HepG2 cells. It is found that 5-demethylnobiletin and NOB, the positive control, elevated DiI-LDL uptake remarkably as shown by fluorescence microscopy (Fig. 8A). Flow cytometry analysis was then employed to quantitate the LDLR activity of treated HepG2 cells. Figure 8B shows that NOB and 5-demethylnobiletin enhance 1.3- and 1.5-fold LDL uptake, respectively, compared with vehicle control.

To investigate whether the increased LDLR binding activity was related to the enhanced gene expression, LDLR mRNA expression was analyzed by RT-Q-PCR. Figure 9A shows that both NOB and 5-demethylnobiletin exhibited an inverted-U dose–response induction [24], with peak induction of 3.9- and 3.3-fold of control ($p<0.01$) at 10 μM, respectively.

3.6 Effect of 5-demethylnobiletin on HMG-CoA reductase mRNA expression

The expression of LDLR and HMG-CoA reductase, the key enzyme of cholesterol biosynthesis pathway, was regulated

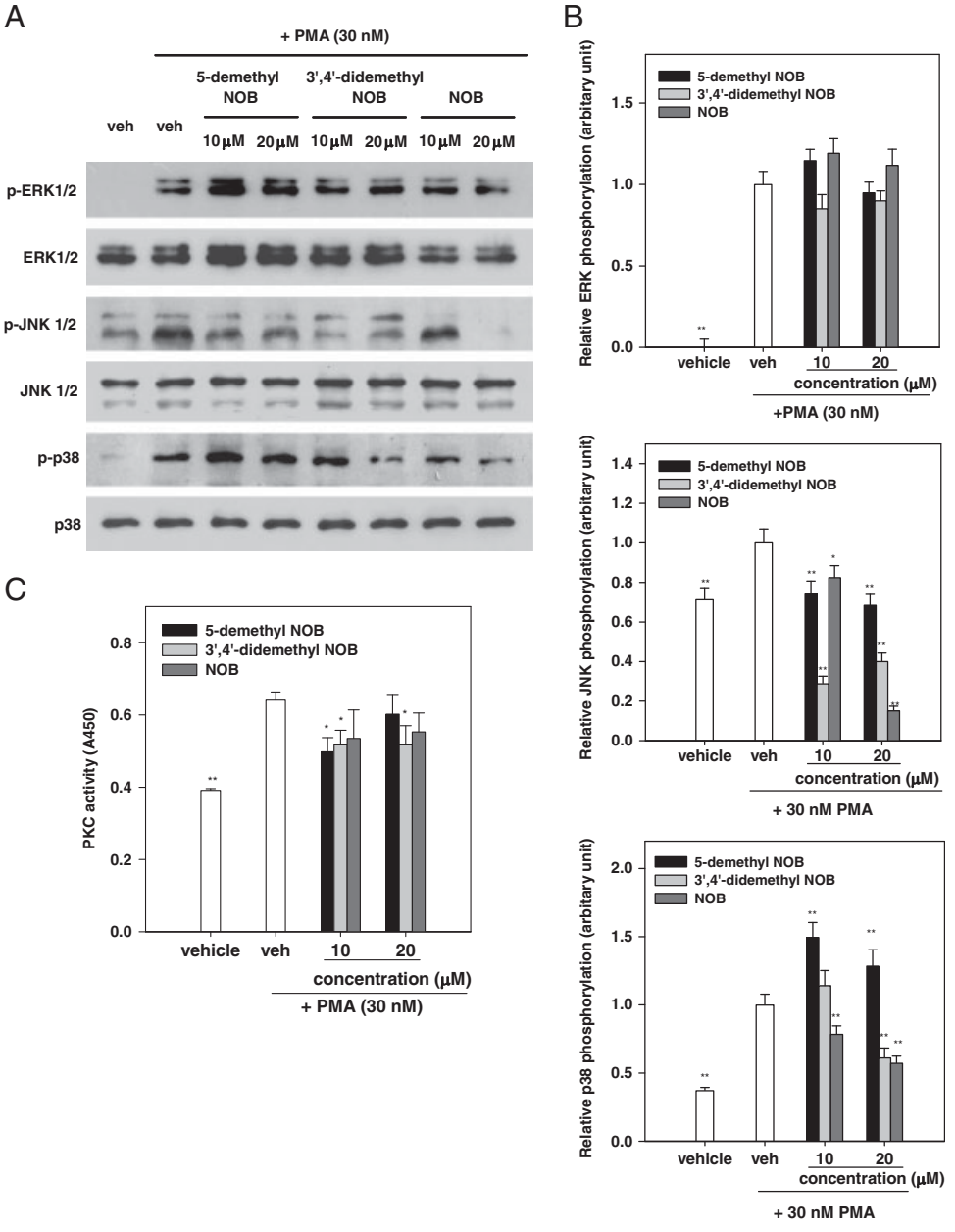

Figure 5. Effects of 5-demethylnobiletin, 3′,4′-didemethylnobiletin, and NOB on the activation of ERK1/2, JNK, and p38 MAPK and PKC in PMA-stimulated THP-1 monocytes. THP-1 monocytes were incubated with the indicated agent or vehicle (0.1% DMSO, v/v) for 30 min and then stimulated with PMA (30 nM) for 2 h. Specific phospho-MAPK proteins were detected in whole-cell lysates by Western blot. Probing for ERK1/2, JNK, and p38 served as an internal loading control (A). Data points that represent the normalized intensities of phosphorylated MAPKs (p-MAPKs) *versus* nonphosphorylated MAPKs are presented as mean ratio ± SEM of three independent experiments relative to the value of vehicle plus PMA (B). PKC activity in the samples was analyzed by a nonradioactive PKC activity assay kit (Enzo Life Sciences) (C). Data represent mean ± SEM of three independent experiments. $^{*}p<0.05$ and $^{**}p<0.01$ represent significant differences compared with vehicle plus PMA.

predominantly at the transcriptional level through a negative feedback control by the intracellular cholesterol. The control is through the interaction between the sterol-regulatory element (SRE) in the promoter and SREBP [60]. Citrus flavonoids, hesperetin, and NOB have been reported to stimulate SRE-containing LDLR promoter activity [24], and as a result, it would be plausible that 5-demethylnobiletin may also affect the mRNA expression of HMG-CoA reductase. Figure 9B shows that HepG2 cells incubated with NOB and 5-demethylnobiletin enhanced HMG-CoA reductase mRNA expression with a similar inverted-U dose response as described above for LDLR expression (Fig. 9A). A total of 10 μM NOB and 5-demethylnobiletin significantly induced HMG-CoA reductase mRNA expression by 3.2- and 2.8-folds, respectively, ($p<0.01$).

3.7 Effect of 5-demethylnobiletin on SREBP-2 processing

Given that the expression of two SREBP-2 target genes (LDLR and HMG-CoA reductase) responded similarly to changing concentration of NOB and 5-demethylnobiletin (Fig. 9A and B), we sought more direct evidence that this effect was mediated by SREBP-2 transcription factor. Since the IgG-1C6 anti-SREBP-2 antibody binds to the *C*-terminus

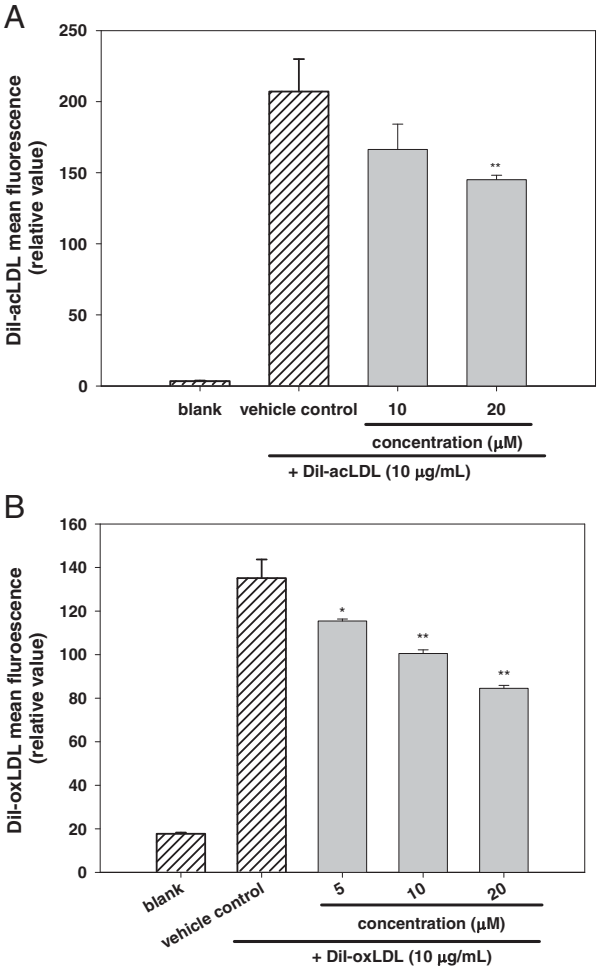

Figure 6. Effects of 5-demethylnobiletin on the uptake of Dil-acLDL (A) and Dil-oxLDL (B) in THP-1-derived macrophages. THP-1-derived macrophages which were pretreated with the indicated concentration of 5-demethylnobiletin for 48 h were incubated with Dil-modified LDL (10 μg/mL) for additional 24 h. The uptake of Dil-modified LDL was quantitated by flow cytometry and expressed as the geometric mean fluorescence intensity. Results are presented as mean ± SEM of three independent experiments. $^{*}p < 0.05$ and $^{**}p < 0.01$ represent significant differences compared with vehicle control of THP-1-derived macrophages.

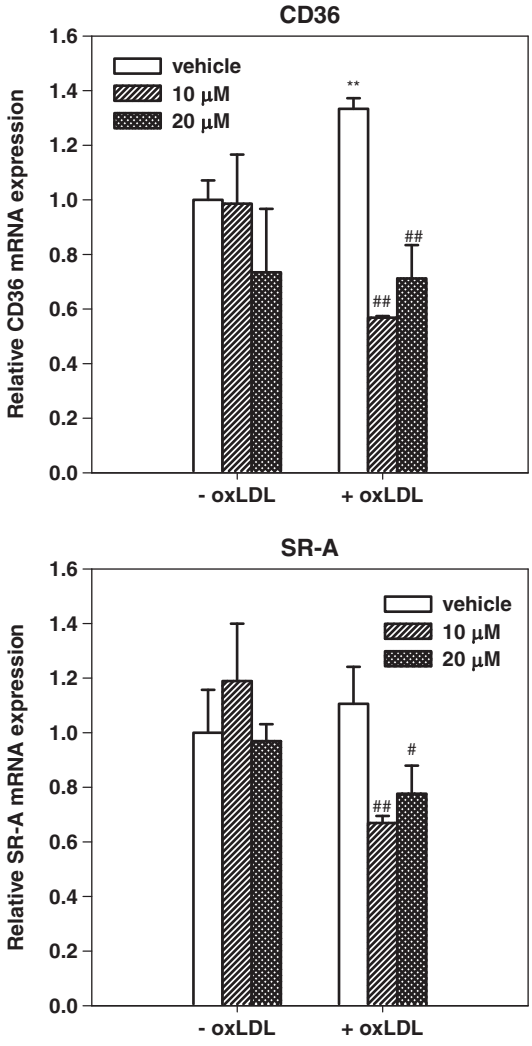

Figure 7. Effect of 5-demethylnobiletin on the mRNA expression of CD36 and SR-A in THP-1-derived macrophages. THP-1-derived macrophages were treated with vehicle (0.1% DMSO) or the indicated concentration of 5-demethylnobiletin in the presence or absence of oxLDL (25 μg/mL) for 48 h. Total cellular RNA was prepared and the expression of mRNA was analyzed as described in Section 2. The data were normalized with reference to the expression levels of the corresponding GAPDH mRNAs. Data represent the mean ratio ± SEM of three independent experiments relative to the value of vehicle control in the absence of oxLDL. $^{**}p < 0.01$ represents significant differences compared with vehicle control in the absence of oxLDL. $^{\#}p < 0.05$ and $^{\#\#}p < 0.01$ represent significant differences compared with vehicle in the presence of oxLDL.

[61], it detects the *C*-terminal cleavage product, giving an indication of SREBP-2 processing [62]. Figure 9C shows the immunoblot assay of *C*-terminal cleavage product of SREBP-2 protein (~62 kDa) in total HepG2 cell lysates. We found that NOB and 5-demethylnobiletin (10 μM) significantly increased SREBP-2 cleavage as compared with normal vehicle. In addition, we assessed the level of nuclear mature SREBP-2 with another antibody that recognizes the amino-terminal transcription factor domain. It was found that NOB and 5-demethylnobiletin (10 μM) increased the content of mature SREBP-2 protein (~68 kDa) in HepG2 nucleus (Fig. 9D).

3.8 Effect of 5-demethylnobiletin on DGAT2 mRNA expression in HepG2 cells

The availability of lipid, particularly triacylglycerols, is widely accepted as a major contributing factor in the regulation of apoB-containing lipoprotein assembly and secretion in HepG2 cells [63]. To investigate whether 5-demethylnobiletin might affect triacylglycerol biosynthesis, the mRNA

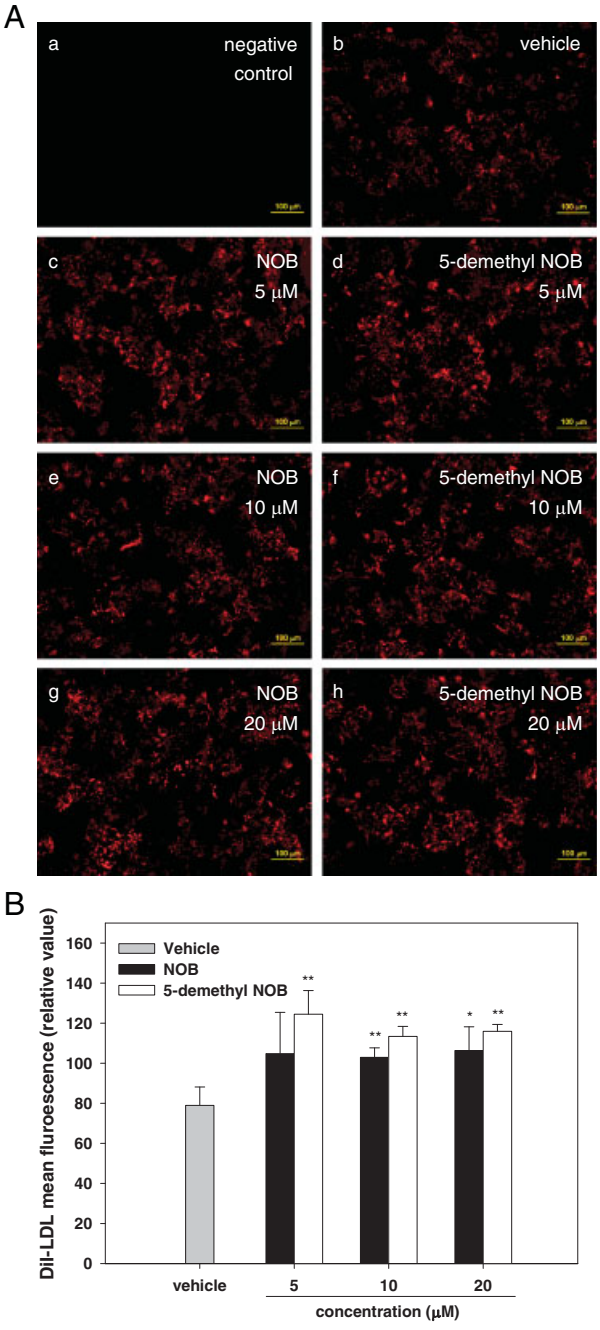

Figure 8. Effects of NOB and 5-demethylnobiletin on LDLR activity. HepG2 cells (1×10^6/mL) were seeded in 6-well plates for 24 h for attachment, and then changed to serum-free medium for overnight. Cells were then treated with the indicated compound or control vehicle (0.1% v/v DMSO) for 24 h. DiI-LDL (10 μg/mL) was then added and incubated for 24 h. Cell association of DiI-LDL was observed under fluorescence microscopy (A). Cells were then analyzed by flow cytometry and expressed as the geometric mean fluorescence intensity (B). $^{*}p<0.05$ and $^{**}p<0.01$ represent significant differences compared with vehicle control.

expression of the key enzyme, DGAT2, was analyzed. Figure 9E shows that NOB and 5-demethylnobiletin inhibited DGAT2 expression by about 30–45%.

4 Discussion

Citrus flavonoids are hypothesized to reduce the occurrence of coronary heart disease through their ability to reduce plasma cholesterol concentrations and inhibit macrophage-derived foam cell formation [26–28]. In this study, we first used PMA-stimulated THP-1 cells as a model to study the effect of 5-demethylnobiletin on gene expression associated with macrophage differentiation. Noncytotoxic concentration of 5-demethylnobiletin (up to 20 μM) could significantly reduce the transcripts of SRs, LOX-1, SR-A, and CD36, in a dose-dependent manner (Fig. 2B–D). However, the expression of adhesion molecule CD11b, which plays an important role in monocyte adherence to endothelial cell [64], was not altered (Fig. 2A). This result indicates that PMA-induced expression of CD11b and SRs is differentially regulated by 5-demethylnobiletin. As a result, 5-demethylnobiletin may be potent in preventing SR-mediated modified LDL uptake rather than in reducing CD11b-dependent monocyte recruitment in atherogenesis. Indeed, treatment of THP-1 cells with 5-demethylnobiletin (5–10 μM) during differentiation dose dependently reduced PMA-stimulated uptake of acLDL (Fig. 3B) and this effect may result from the combined decrease in SR-A and CD36 expression (Fig. 2C and D).

With regard to other structure-relevant PMFs, it was found that NOB, a permethoxylated PMF, suppressed only the expression of LOX-1 but had no effect on that of CD11b or SR-A in PMA-treated THP-1 cells. On the other hand, 3′,4′-didemethylnobiletin, a dihydroxylated PMF, strongly reduced expression of CD11b and SRs during macrophage differentiation. Furthermore, PMA-stimulated DiI-acLDL uptake was also significantly attenuated by 3′,4′-didemethylnobiletin, but only modestly inhibited by NOB (Supporting Information Table 2). These data indicate that the hydroxyl groups of PMF may play a vital role in down-regulation of PMA-induced SR expression and activity so that demethylated PMFs exert stronger suppressive effect than its permethoxylated counterpart.

Both NF-κB and AP-1 are PMA-inducible nuclear factors [65]. AP-1 is a dimeric complex composed of members of the Fos and Jun proteins [66]. AP-1 binding sites are found in the 5′ flanking regions of LOX-1 [51] and SR-A [67]. NF-κB binding site-like sequences also exist in LOX-1 [51] and CD36 [68] genes and NF-κB activation is implicated in the regulation of gene expression crucial for progression of atherogenesis [69]. Previous studies have suggested that AP-1 and NF-κB have a critical role in PMA-induced SR expression [30]; in agreement, we found that PMA increased the DNA-binding activity of both AP-1 and NF-κB in EMSA experiment. With respect to PMA-induced AP-1 and NF-κB activation, 5-demethylnobiletin (10 and 20 μM) was

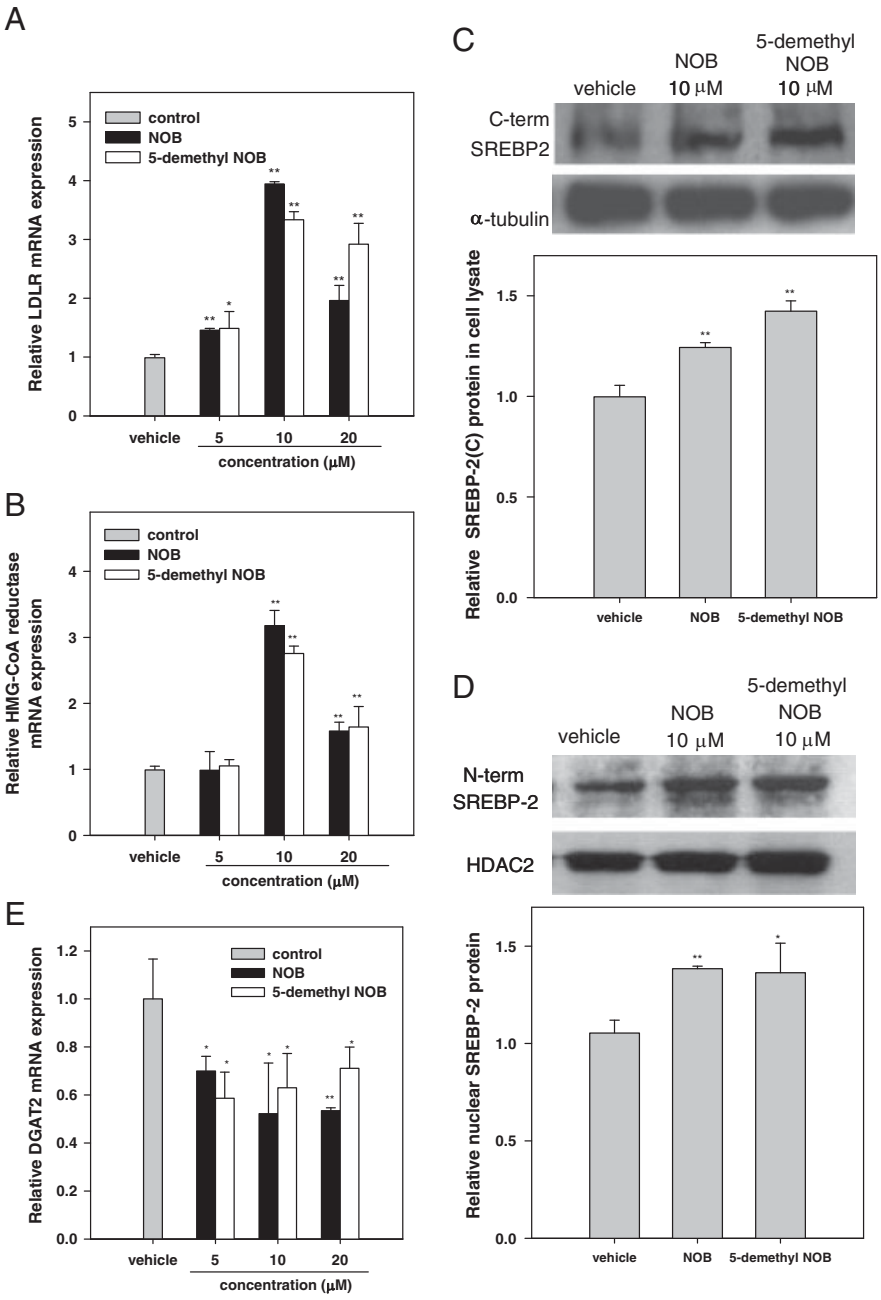

Figure 9. Effects of NOB and 5-demethylnobiletin on the mRNA expression of LDLR (A), HMG-CoA reductase (B), DGAT2 (E), and SREBP-2 processing (C and D). HepG2 cells (1×10^6/mL) were seeded in 6-well plates for 24 h in normal medium and then treated with the indicated compound or control vehicle (0.1% v/v DMSO) for 24 h. Total cellular RNA was prepared and the expression of specific gene was analyzed as described in Section 2. The data were normalized with reference to the expression levels of the corresponding GAPDH mRNAs. Data represent mean ratio $\pm$ SEM of three independent experiments relative to the value of vehicle control. $^{*}p<0.05$ and $^{**}p<0.01$ represent significant differences compared with vehicle control (A, B, and E). Total cell lysates of 30 μg protein *per* sample were used to detect the C-terminal fragment of the cleavage SREBP-2 (~62 kDa) by Western blotting with the IgG-1C6 anti-SREBP-2 antibody. Probing for α-tubulin served as an internal loading control. Data points that represent the normalized intensities of C-terminus of SREBP-2 *versus* α-tubulin are presented as mean ratio $\pm$ SEM of three independent experiments relative to the value of vehicle control. $^{**}p<0.01$ represents significant difference compared with vehicle control (C). Nuclear extracts of 30 μg protein *per* sample were used to detect the mature form of SREBP-2 (~68 kDa) with the anti-SREBP-2 (amino acids 455–469) antibody. Probing for histone deacetylase 2 (HDAC2) served as an internal loading control. Data points that represent the normalized intensities of *N*-terminus of SREBP-2 *versus* HDAC2 are presented as mean ratio $\pm$ SEM of three independent experiments relative to the value of vehicle control. $^{*}p<0.05$ and $^{**}p<0.01$ represent significant differences compared with vehicle control (D).

found to downregulate the former more effectively, but produce modest effect on the latter. On the other hand, the positive control, 3′,4′-didemethylnobiletin, exerted effective effect on both nuclear factors (Fig. 4). In parallel with the reduction in SR transcript, current data suggest that 5-demethylnobiletin exerted its anti-SR expression *via* NF-κB- and AP-1-dependent pathways.

The MAPKs are a family of second messenger kinases that are essential for transferring signals from the cell surface to the nucleus. ERK, JNK, and p38 MAPK-mediated signaling pathways have been associated with AP-1 [70–72] and NF-κB activation. PMA, a direct activator of PKC, is a strong MAPK stimulator [73, 74]; in agreement, we found that PMA stimulated marked activation of ERK1/2, JNK1/2, and p38 MAPK (Fig. 5A). 5-Demethylnobiletin, 3′,4′-didemethylnobiletin, and NOB inhibited the PMA-induced phosphorylation of JNK1/2 but not ERK (Fig. 5A). However, their effects on the phosphorylation of p38 MAPK did not correlated with those of NF-κB, AP-1 activities, or SR expression. Furthermore, 5-demethylnobiletin and 3′,4′-didemethylnobiletin, but not NOB, were able to significantly inhibit PMA-induced PKC activity (Fig. 5C). These results suggested that 5-demethylnobiletin interferes with PKC and JN signalings, which might affect activation of NF-κB and AP-1 and subsequent SR expression in PMA-induced THP-1 cells.

We further questioned whether 5-demethylnobiletin also inhibited foam cell formation in THP-1-derived macrophages. Figure 7 shows that 5-demethylnobiletin does not change the basal expression of CD36 or SR-A in macrophages. This result differed from those of NOB and 3′,4′-didemethylnobiletin, which could downregulate mRNA level of SRs in THP-1-derived macrophages (Supporting Information Table 3) [31]. When THP-1-derived macrophages were treated with oxLDL (25 μg/mL), only CD36, but not SR-A, was upregulated. This result coincides with that by Tsukamoto *et al*. [59], who reported that SR-A expression was not changed during foam cell formation. 5-Demethylnobiletin significantly repressed SR-A and CD36 mRNA expression in THP-1-derived macrophages which were coincubated with oxLDL (Fig. 7).

5-Demethylnobiletin, 3′,4′-didemethylnobiletin, and NOB markedly inhibited both DiI-modified LDL uptake in THP-1-derived macrophages in a dose-dependent manner (Fig. 6 and Supporting Information Table 3). Among these three PMFs, 3′,4′-didemethylnobiletin appears to be the most potent followed by 5-demethylnobiletin and NOB. Due to the lack of strong correlation between the mRNA expression (Fig. 7) and the activity (Fig. 6) of SRs, we conclude that the attenuation of modified LDL uptake in THP-1-derived macrophages may not be caused by mere downregulation of SRs; it is likely that these PMFs function as downstream of SR ligand binding as well.

To investigate the potential hypolipidemic effect of 5-demethylnobiletin, we first studied its effect on LDLR activity in HepG2 cells. It is well known that DiI-LDL uptake activity was reduced in the presence of unlabelled LDL [75]; as a result, serum-free or LDL-free medium was employed during the uptake analysis [44]. Fluorescence microscope (Fig. 8A) and flow cytometry (Fig. 8B) provide live-cell imaging and numeric data of increased DiI-fluorescence intensity in both NOB- and 5-demethylnobiletin-treated HepG2 cells, indicating that they are potent to augment LDLR activity.

We next examined whether LDLR mRNA levels were affected by 5-demethylnobiletin. It has been suggested that to ensure basal levels of SREBP available to mediate flavonoid action, the cells should remain in normal medium [24]. RT-Q-PCR data revealed that NOB and 5-demethylnobiletin (10 μM) stimulated LDLR expression by more than threefold as compared with vehicle control (Fig. 9A). This result is similar to that by Morin *et al*. [24], who reported that NOB upregulated LDLR expression with compatible potency and efficacy by SRE-mediated reporter analysis.

In addition to LDLR, cholesterol balance is also maintained in the cells by sterol-mediated feedback repression of several other genes including HMG-CoA reductase, which is involved in the synthetic pathway of cholesterol. The mechanism for this dual regulation is through the control of SREBPs [60]. NOB and 5-demethylnobiletin were found strongly upregulated HMG-CoA reductase gene expression with a similar hormetic dose response as for LDLR expression (Fig. 9) and increased the level of C-terminal cleavage product of SREBP-2 in total cell lysates (Fig. 9C), in conjugation with enhanced level of nuclear amino terminus of SREBP-2 (Fig. 9D). These results indicate that the processing of SREBP-2, a common transcriptional factor for LDLR and HMG-CoA reductase, was activated by NOB and 5-demethylnobiletin.

Hypertriglyceridemia plays a crucial role in the development of atherosclerosis and a major contributor is the hepatic overproduction of VLDL [14]. The final and the only committed step in the biosynthesis of triacylglycerols is catalyzed by DGAT enzymes. In this research, we showed, for the first time, that NOB and 5-demethylnobiletin inhibited DGAT2 mRNA expression significantly. As a consequence, enhanced LDLR and reduced DGAT2 expression, together with the previous findings of reduced activity and expression of acyl CoA: cholesterol acyl-CoA: cholesterol acyltransferase and microsomal triglyceride transfer protein [26], might be associated with the hypolipidemic properties of the citrus flavonoids.

In conclusion, this study investigated, for the first time, the anti-atherosclerotic action and underlying mechanism of 5-demethylnobiletin in cell-culture system. We found that there are several mechanisms at work in parallel for the effect of 5-demethylnobiletin. It attenuates monocyte differentiation into macrophage and blunts foam cell formation by downregulating SR expression and activity. In addition, 5-demethylnobiletin also alters the lipid homeostasis in hepatocytes by upregulating LDLR expression *via* SREBP-2 activation and by downregulating DGAT2 expression.

This research was supported by Grants NSC-97-2320-B-320-011-MY3 (to Dr. J.-H. Yen) and NSC-96-2320-B-041-006-MY3 (to Dr. M.-J. Wu) from the National Science Council and Campus Integrated Project Grant (to Dr. M.-J. Wu) from Chia Nan University, Taiwan.

The authors have declared no conflict of interest.

5 References

[1] Libby, P., Inflammation in atherosclerosis. *Nature* 2002, *420*, 868–874.

[2] Navab, M., Imes, S. S., Hama, S. Y., Hough, G. P. *et al.*, Monocyte transmigration induced by modification of low density lipoprotein in cocultures of human aortic wall cells is due to induction of monocyte chemotactic protein 1 synthesis and is abolished by high density lipoprotein. *J. Clin. Invest.* 1991, *88*, 2039–2046.

[3] Yamada, Y., Doi, T., Hamakubo, T., Kodama, T., Scavenger receptor family proteins: roles for atherosclerosis, host defence and disorders of the central nervous system. *Cell. Mol. Life Sci.* 1998, *54*, 628–640.

[4] de Villiers, W. J., Smart, E. J., Macrophage scavenger receptors and foam cell formation. *J. Leukoc. Biol.* 1999, *66*, 740–746.

[5] Febbraio, M., Podrez, E. A., Smith, J. D., Hajjar, D. P. *et al.*, Targeted disruption of the class B scavenger receptor CD36 protects against atherosclerotic lesion development in mice. *J. Clin. Invest.* 2000, *105*, 1049–1056.

[6] Suzuki, H., Kurihara, Y., Takeya, M., Kamada, N. *et al.*, A role for macrophage scavenger receptors in atherosclerosis and susceptibility to infection. *Nature* 1997, *386*, 292–296.

[7] Babaev, V. R., Gleaves, L. A., Carter, K. J., Suzuki, H. *et al.*, Reduced atherosclerotic lesions in mice deficient for total or macrophage-specific expression of scavenger receptor-A. *Arterioscler. Thromb. Vasc. Biol.* 2000, *20*, 2593–2599.

[8] Sakaguchi, H., Takeya, M., Suzuki, H., Hakamata, H. *et al.*, Role of macrophage scavenger receptors in diet-induced atherosclerosis in mice. *Lab. Invest.* 1998, *78*, 423–434.

[9] Mehta, J. L., Sanada, N., Hu, C. P., Chen, J. *et al.*, Deletion of LOX-1 reduces atherogenesis in LDLR knockout mice fed high cholesterol diet. *Circ. Res.* 2007, *100*, 1634–1642.

[10] Hu, C., Chen, J., Dandapat, A., Fujita, Y. *et al.*, LOX-1 abrogation reduces myocardial ischemia-reperfusion injury in mice. *J. Mol. Cell. Cardiol.* 2008, *44*, 76–83.

[11] Brown, M. S., Goldstein, J. L., A receptor-mediated pathway for cholesterol homeostasis. *Science* 1986, *232*, 34–47.

[12] Scharnagl, H., Marz, W., New lipid-lowering agents acting on LDL receptors. *Curr. Top. Med. Chem.* 2005, *5*, 233–242.

[13] Kong, W., Wei, J., Abidi, P., Lin, M. *et al.*, Berberine is a novel cholesterol-lowering drug working through a unique mechanism distinct from statins. *Nat. Med.* 2004, *10*, 1344–1351.

[14] Phillips, N., Waters, D., Havel, R., Plasma lipoproteins and progression of coronary artery disease evaluated by angiography and clinical events. *Circulation* 1993, *88*, 2762–2770.

[15] Benoist, F., Grand-Perret, T., ApoB-100 secretion by HepG2 cells is regulated by the rate of triglyceride biosynthesis but not by intracellular lipid pools. *Arterioscler. Thromb. Vasc. Biol.* 1996, *16*, 1229–1235.

[16] Cases, S., Stone, S. J., Zhou, P., Yen, E. *et al.*, Cloning of DGAT2, a second mammalian diacylglycerol acyltransferase, and related family members. *J. Biol. Chem.* 2001, *276*, 38870–38876.

[17] Tripoli, E., Guardia, M. L., Giammanco, S., Majo, D. D., Giammanco, M., Citrus flavonoids: molecular structure, biological activity and nutritional properties: a review. *Food Chem.* 2007, *104*, 466–479.

[18] Jeon, S. M., Park, Y. B., Choi, M. S., Antihypercholesterolemic property of naringin alters plasma and tissue lipids, cholesterol-regulating enzymes, fecal sterol and tissue morphology in rabbits. *Clin. Nutr.* 2004, *23*, 1025–1034.

[19] Kim, S. Y., Kim, H. J., Lee, M. K., Jeon, S. M. *et al.*, Naringin time-dependently lowers hepatic cholesterol biosynthesis and plasma cholesterol in rats fed high-fat and high-cholesterol diet. *J. Med. Food* 2006, *9*, 582–586.

[20] Bok, S. H., Lee, S. H., Park, Y. B., Bae, K. H. *et al.*, Plasma and hepatic cholesterol and hepatic activities of 3-hydroxy-3-methyl-glutaryl-CoA reductase and acyl CoA: cholesterol transferase are lower in rats fed citrus peel extract or a mixture of citrus bioflavonoids. *J. Nutr.* 1999, *129*, 1182–1185.

[21] Kurowska, E. M., Manthey, J. A., Hypolipidemic effects and absorption of citrus polymethoxylated flavones in hamsters with diet-induced hypercholesterolemia. *J. Agric. Food Chem.* 2004, *52*, 2879–2886.

[22] Chiba, H., Uehara, M., Wu, J., Wang, X. *et al.*, Hesperidin, a citrus flavonoid, inhibits bone loss and decreases serum and hepatic lipids in ovariectomized mice. *J. Nutr.* 2003, *133*, 1892–1897.

[23] Jung, U. J., Kim, H. J., Lee, J. S., Lee, M. K. *et al.*, Naringin supplementation lowers plasma lipids and enhances erythrocyte antioxidant enzyme activities in hypercholesterolemic subjects. *Clin. Nutr.* 2003, *22*, 561–568.

[24] Morin, B., Nichols, L. A., Zalasky, K. M., Davis, J. W. *et al.*, The citrus flavonoids hesperetin and nobiletin differentially regulate low density lipoprotein receptor gene transcription in HepG2 liver cells. *J. Nutr.* 2008, *138*, 1274–1281.

[25] Kurowska, E., Manthey, J., Casaschi, A., Theriault, A., Modulation of hepG2 cell net apolipoprotein B secretion by the citrus polymethoxyflavone, tangeretin. *Lipids* 2004, *39*, 143–151.

[26] Wilcox, L. J., Borradaile, N. M., de Dreu, L. E., Huff, M. W., Secretion of hepatocyte apoB is inhibited by the flavonoids, naringenin and hesperetin, via reduced activity and expression of ACAT2 and MTP. *J. Lipid Res.* 2001, *42*, 725–734.

[27] Lee, C. H., Jeong, T. S., Choi, Y. K., Hyun, B. H. *et al.*, Anti-atherogenic effect of citrus flavonoids, naringin and

naringenin, associated with hepatic ACAT and aortic VCAM-1 and MCP-1 in high cholesterol-fed rabbits. *Biochem. Biophys. Res. Commun.* 2001, *284*, 681–688.

[28] Whitman, S. C., Kurowska, E. M., Manthey, J. A., Daugherty, A., Nobiletin, a citrus flavonoid isolated from tangerines, selectively inhibits class A scavenger receptor-mediated metabolism of acetylated LDL by mouse macrophages. *Atherosclerosis* 2005, *178*, 25–32.

[29] Eguchi, A., Murakami, A., Ohigashi, H., Nobiletin, a citrus flavonoid, suppresses phorbol ester-induced expression of multiple scavenger receptor genes in THP-1 human monocytic cells. *FEBS Lett.* 2006, *580*, 3321–3328.

[30] Eguchi, A., Murakami, A., Li, S., Ho, C. T., Ohigashi, H., Suppressive effects of demethylated metabolites of nobiletin on phorbol ester-induced expression of scavenger receptor genes in THP-1 human monocytic cells. *Biofactors* 2007, *31*, 107–116.

[31] Lo, Y. H., Pan, M. H., Li, S., Yen, J. H. *et al.*, Nobiletin metabolite, 3′,4′-dihydroxy-5,6,7,8-tetramethoxyflavone, inhibits LDL oxidation and down-regulates scavenger receptor expression and activity in THP-1 cells. *Biochim. Biophys. Acta* 2010, *1801*, 114–126.

[32] Li, S., Lo, C. Y., Ho, C. T., Hydroxylated polymethoxyflavones and methylated flavonoids in sweet orange (*Citrus sinensis*) peel. *J. Agric. Food Chem.* 2006, *54*, 4176–4185.

[33] Li, S., Pan, M. H., Lai, C. S., Lo, C. Y. *et al.*, Isolation and syntheses of polymethoxyflavones and hydroxylated polymethoxyflavones as inhibitors of HL-60 cell lines. *Bioorg. Med. Chem.* 2007, *15*, 3381–3389.

[34] Xiao, H., Yang, C. S., Li, S., Jin, H. *et al.*, Monodemethylated polymethoxyflavones from sweet orange (*Citrus sinensis*) peel inhibit growth of human lung cancer cells by apoptosis. *Mol. Nutr. Food Res.* 2009, *53*, 398–406.

[35] Qiu, P., Dong, P., Guan, H., Li, S. *et al.*, Inhibitory effects of 5-hydroxy polymethoxyflavones on colon cancer cells. *Mol. Nutr. Food Res.* 2010.

[36] Pan, M. H., Lai, Y. S., Lai, C. S., Wang, Y. J. *et al.*, 5-Hydroxy-3,6,7,8,3′,4′-hexamethoxyflavone induces apoptosis through reactive oxygen species production, growth arrest and DNA damage-inducible gene 153 expression, and caspase activation in human leukemia cells. *J. Agric. Food Chem.* 2007, *55*, 5081–5091.

[37] Li, S., Sang, S., Pan, M. H., Lai, C. S. *et al.*, Anti-inflammatory property of the urinary metabolites of nobiletin in mouse. *Bioorg. Med. Chem. Lett.* 2007, *17*, 5177–5181.

[38] Gotto, A. M., Jr., Pownall, H. J., Havel, R. J., Introduction to the plasma lipoproteins. *Meth. Enzymol.* 1986, *128*, 3–41.

[39] Bradford, M. M., A rapid and sensitive method for the quantitation of microgram quantities of protein utilizing the principle of protein-dye binding. *Anal. Biochem.* 1976, *72*, 248–254.

[40] Hermann, M., Gmeiner, B., Altered susceptibility to *in vitro* oxidation of LDL in LDL complexes and LDL aggregates. *Ann. N.Y. Acad. Sci.* 1993, *683*, 363–364.

[41] Teupser, D., Thiery, J., Walli, A. K., Seidel, D., Determination of LDL- and scavenger-receptor activity in adherent and non-adherent cultured cells with a new single-step fluorometric assay. *Biochim. Biophys. Acta* 1996, *1303*, 193–198.

[42] Devaraj, S., Hugou, I., Jialal, I., Alpha-tocopherol decreases CD36 expression in human monocyte-derived macrophages. *J. Lipid Res.* 2001, *42*, 521–527.

[43] Basu, S. K., Goldstein, J. L., Anderson, G. W., Brown, M. S., Degradation of cationized low density lipoprotein and regulation of cholesterol metabolism in homozygous familial hypercholesterolemia fibroblasts. *Proc. Natl. Acad. Sci. USA* 1976, *73*, 3178–3182.

[44] Mullen, E., Brown, R. M., Osborne, T. F., Shay, N. F., Soy isoflavones affect sterol regulatory element binding proteins (SREBPs) and SREBP-regulated genes in HepG2 cells. *J. Nutr.* 2004, *134*, 2942–2947.

[45] Carmichael, J., DeGraff, W. G., Gazdar, A. F., Minna, J. D., Mitchell, J. B., Evaluation of a tetrazolium-based semiautomated colorimetric assay: assessment of chemosensitivity testing. *Cancer Res.* 1987, *47*, 936–942.

[46] Wang, X., Seed, B., A PCR primer bank for quantitative gene expression analysis. *Nucl. Acids Res.* 2003, *31*, e154.

[47] Carter, A. B., Tephly, L. A., Hunninghake, G. W., The absence of activator protein 1-dependent gene expression in THP-1 macrophages stimulated with phorbol esters is due to lack of p38 mitogen-activated protein kinase activation. *J. Biol. Chem.* 2001, *276*, 33826–33832.

[48] Tuomisto, T. T., Riekkinen, M. S., Viita, H., Levonen, A. L., Yla-Herttuala, S., Analysis of gene and protein expression during monocyte-macrophage differentiation and cholesterol loading – cDNA and protein array study. *Atherosclerosis* 2005, *180*, 283–291.

[49] Wang, Y., Zhang, J., Dai, W., Lei, K., Pike, J., Dexamethasone potently enhances phorbol ester-induced IL-1beta gene expression and nuclear factor NF-kappaB activation. *J. Immunol.* 1997, *159*, 534–537.

[50] Serkkola, E., Hurme, M., Synergism between protein-kinase C and cAMP-dependent pathways in the expression of the interleukin-1 beta gene is mediated via the activator-protein-1 (AP-1) enhancer activity. *Eur. J. Biochem.* 1993, *213*, 243–249.

[51] Nagase, M., Abe, J., Takahashi, K., Ando, J. *et al.*, Genomic organization and regulation of expression of the lectin-like oxidized low-density lipoprotein receptor (LOX-1) gene. *J. Biol. Chem.* 1998, *273*, 33702–33707.

[52] Kaufman, P. A., Weinberg, J. B., Greene, W. C., Nuclear expression of the 50- and 65-kD Rel-related subunits of nuclear factor-kappa B is differentially regulated in human monocytic cells. *J. Clin. Invest.* 1992, *90*, 121–129.

[53] Shen, G., Jeong, W. S., Hu, R., Kong, A. N., Regulation of Nrf2, NF-kappaB, and AP-1 signaling pathways by chemopreventive agents. *Antioxid. Redox. Signal.* 2005, *7*, 1648–1663.

[54] Janssens, S., Beyaert, R., Functional diversity and regulation of different interleukin-1 receptor-associated kinase (IRAK) family members. *Mol. Cell* 2003, *11*, 293–302.

[55] Viatour, P., Merville, M. P., Bours, V., Chariot, A., Phosphorylation of NF-kappaB and IkappaB proteins: implica-

tions in cancer and inflammation. *Trends Biochem. Sci.* 2005, *30*, 43–52.

[56] Chang, Z. L., Beezhold, D. H., Protein kinase C activation in human monocytes: regulation of PKC isoforms. *Immunology* 1993, *80*, 360–366.

[57] Han, S., Sidell, N., Peroxisome-proliferator-activated-receptor gamma (PPARgamma) independent induction of CD36 in THP-1 monocytes by retinoic acid. *Immunology* 2002, *106*, 53–59.

[58] Kunjathoor, V. V., Febbraio, M., Podrez, E. A., Moore, K. J. *et al.*, Scavenger receptors class A-I/II and CD36 are the principal receptors responsible for the uptake of modified low density lipoprotein leading to lipid loading in macrophages. *J. Biol. Chem.* 2002, *277*, 49982–49988.

[59] Tsukamoto, K., Kinoshita, M., Kojima, K., Mikuni, Y. *et al.*, Synergically increased expression of CD36, CLA-1 and CD68, but not of SR-A and LOX-1, with the progression to foam cells from macrophages. *J. Atheroscler. Thromb.* 2002, *9*, 57–64.

[60] Brown, M. S., Goldstein, J. L., Cholesterol feedback: from Schoenheimer's bottle to Scap's MELADL. *J. Lipid Res.* 2009, *50*, S15–S27.

[61] Hua, X., Sakai, J., Ho, Y. K., Goldstein, J. L., Brown, M. S., Hairpin orientation of sterol regulatory element-binding protein-2 in cell membranes as determined by protease protection. *J. Biol. Chem.* 1995, *270*, 29422–29427.

[62] Krycer, J. R., Kristiana, I., Brown, A. J., Cholesterol homeostasis in two commonly used human prostate cancer cell-lines, LNCaP and PC-3. *PLoS ONE* 2009, *4*, e8496.

[63] Wu, X., Sakata, N., Lui, E., Ginsberg, H. N., Evidence for a lack of regulation of the assembly and secretion of apolipoprotein B-containing lipoprotein from HepG2 cells by cholesteryl ester. *J. Biol. Chem.* 1994, *269*, 12375–12382.

[64] Miller, L. J., Schwarting, R., Springer, T. A., Regulated expression of the Mac-1, LFA-1, p150,95 glycoprotein family during leukocyte differentiation. *J. Immunol.* 1986, *137*, 2891–2900.

[65] Nelsen, B., Hellman, L., Sen, R., The NF-kappa B-binding site mediates phorbol ester-inducible transcription in nonlymphoid cells. *Mol. Cell. Biol.* 1988, *8*, 3526–3531.

[66] Angel, P., Karin, M., The role of Jun, Fos and the AP-1 complex in cell-proliferation and transformation. *Biochim. Biophys. Acta* 1991, *1072*, 129–157.

[67] Mietus-Snyder, M., Glass, C. K., Pitas, R. E., Transcriptional activation of scavenger receptor expression in human smooth muscle cells requires AP-1/c-Jun and C/EBP?: both AP-1 binding and JNK activation are induced by phorbol esters and oxidative stress. *Arterioscler. Thromb. Vasc. Biol.* 1998, *18*, 1440–1449.

[68] Armesilla, A. L., Vega, M. A., Structural organization of the gene for human CD36 glycoprotein. *J. Biol. Chem.* 1994, *269*, 18985–18991.

[69] Ferreira, V., van Dijk, K. W., Groen, A. K., Vos, R. M. *et al.*, Macrophage-specific inhibition of NF-kappaB activation reduces foam-cell formation. *Atherosclerosis* 2007, *192*, 283–290.

[70] Minden, A., Lin, A., Smeal, T., Derijard, B. *et al.*, c-Jun N-terminal phosphorylation correlates with activation of the JNK subgroup but not the ERK subgroup of mitogen-activated protein kinases. *Mol. Cell. Biol.* 1994, *14*, 6683–6688.

[71] Frost, J. A., Geppert, T. D., Cobb, M. H., Feramisco, J. R., A requirement for extracellular signal-regulated kinase (ERK) function in the activation of AP-1 by Ha-Ras, phorbol 12-myristate 13-acetate, and serum. *Proc. Natl. Acad. Sci. USA* 1994, *91*, 3844–3848.

[72] DeSilva, D. R., Feeser, W. S., Tancula, E. J., Scherle, P. A., Anergic T cells are defective in both jun NH2-terminal kinase and mitogen-activated protein kinase signaling pathways. *J. Exp. Med.* 1996, *183*, 2017–2023.

[73] Seger, R., Krebs, E. G., The MAPK signaling cascade. *FASEB J.* 1995, *9*, 726–735.

[74] Franklin, C. C., Kraft, A. S., Conditional expression of the mitogen-activated protein kinase (MAPK) phosphatase MKP-1 preferentially inhibits p38 MAPK and stress-activated protein kinase in U937 cells. *J. Biol. Chem.* 1997, *272*, 16917–16923.

[75] Davalos, A., Fernandez-Hernando, C., Cerrato, F., Martinez-Botas, J. *et al.*, Red grape juice polyphenols alter cholesterol homeostasis and increase LDL-receptor activity in human cells *in vitro*. *J. Nutr.* 2006, *136*, 1766–1773.

